

Technological Characterization and Industrial Application of Tunisian Clays from Makthar Area (Central Tunisia) in the Ceramic Industry

Imed Ben Salah^{1*}, Moufida Ben M'Barek Jemai¹, Ali Sdiri², Najet Shimi Slim³,
Mabrouk Boughdiri¹

¹Department of Geology, University of Sciences of Bizerte, Bizerte, Tunisia

²National Engineering School of Sfax, Sfax, Tunisia

³Department of Geology, University of Sciences of Tunis, Tunis, Tunisia

Email: *imed_bensalah@yahoo.fr

Received 3 June 2014; accepted 25 July 2016; published 28 July 2016

Copyright © 2016 by authors and Scientific Research Publishing Inc.

This work is licensed under the Creative Commons Attribution International License (CC BY).

<http://creativecommons.org/licenses/by/4.0/>



Open Access

Abstract

This study focused on the geochemical, mineralogical and technological characterization of clays in Makthar area (Central of Tunisia) of Cretaceous-Paleogene. Its aims are to identify and promote use in the field of ceramics industry. The result of the mineralogical analysis of clays showed a dominance of illite with a percentage higher than 65%, of kaolinite and smectite with percentages of 15%. Geochemical analysis of the major elements of clay showed a SiO₂ content exceeding 29% and a percentage of Al₂O₃ higher than 7.5%. The Fe₂O₃ percentage was ranging from 3% to 8%. The percentage of CaO was between 22.5% and 28% while that of K₂O is 4%. The percentages of SO₄, MgO and NaO₂ were in very small fractions. Granulometric and microgranulometric analysis showed that the clay fraction (<2 μm) varies from 30% to 37%. The plasticity index showed the plasticity character of clays which presented a specific surface area ranging from 112 m²/g to 178 m²/g reflecting illite dominance. Drying behavior indicated that clay mixture had a drying shrinkage less than 7%, while the firing shrinkage didn't exceed 2% giving the possibility of clay using in the ceramics field.

Keywords

Clay Mineral, Mineralogy, Chemical and Physical Properties, Ceramic, Industry

*Corresponding author.

1. Introduction

The study area is located in the Tunisian Atlas (**Figure 1**) marked by a series of grabens in relay NW-SE direction with E-W slip fault extending from the graben of Siliana to Kef [1] [2]. These grabens were considered quaternary age [3] [4] and for other author contemporary Miocene age [5]. These authors considered that accidents EW and NE-SW are the driving mechanism of apparent discrepancy between the different facies elements as defined in the accident affecting Elles syncline.

The selected sections, located in the Northwest region Makthar, have identified three clay units from Cretaceous-Paleogene age often encountered in Tunisia:

- Unit 1 (A Mkt): This is a greenish clay sequence alternating with gray marl fossilized from Santonian-Lower Campanian age.
- Unit 2 (H Mkt): This is a sequence of clay, interspersing with centimeter levels of limestone in its middle part from upper Maastrichtian-Paleocene age.
- Unit 3 (S Mkt): This is a clay series having a thickness of 130 m containing a few levels of calcite from middle to upper Eocene age.

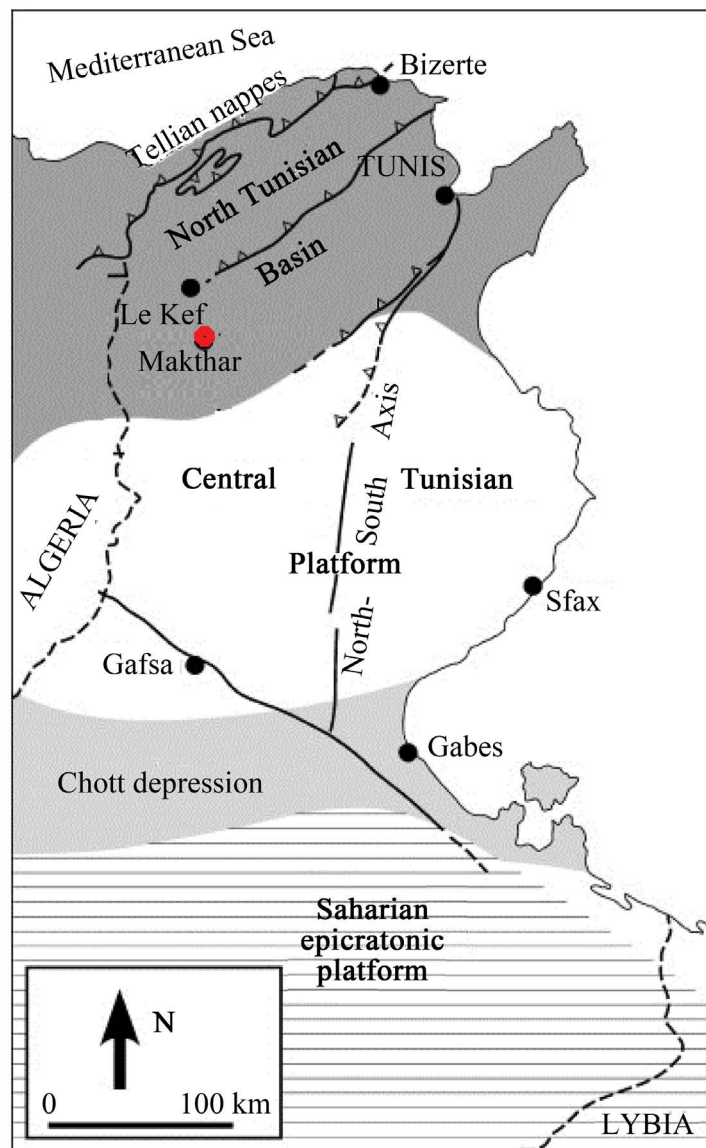


Figure 1. Location of the study area.

The realized studies were carried out on three clay formations, the most representative, taken from clay that outcrops 25 Km from Makthar city to evaluate their potential use in the ceramic field.

2. Materials and Methods

2.1. Mineralogical Study by X-Ray Diffraction

Mineralogical analysis was carried out with a Philips Xpert Pro MD standard beam with copper anti-cathode tube. The mineralogical characterization identifies the percentages of clay minerals ($<2 \mu\text{m}$) and associated minerals [6] [7].

Chemical Analysis

The chemical analysis of major elements was carried out by atomic absorption Perkin Elmer apparatus with acetylene peroxide flame. This analysis allows us to determine the percentages of CaO, Fe₂O₃, Al₂O₃, SiO₂, K₂O, MgO, Na₂O, SO₄, and loss on ignition.

2.2. Granulometric and Micro-Granulometric Analysis

This analysis was carried out under water and the refusal of each sieve was dried and weighed [8]. The micro-size analysis was performed with the Mikromeritics SediGraph 5120 particle size analyzer, size range 0.1 - 300 μm [9]. The particle diameter was determined by measuring the speed of sedimentation of suspended particles according to Stokes law [10].

2.3. Plasticity

Plasticity was determined by the Atterberg limits. Those physical constants define the threshold for passing from a liquid state to a plastic state expressed in water content. Limit liquidity and plastic limit were measured according to the [11]. The plasticity index represents the broad field of plasticity clays [12]. The evaluation of plasticity was performed by Atterberg limits method. The plasticity index was calculated as the arithmetic difference of liquid limit and plastic limit. This analysis was carried out with a Casagrande apparatus.

2.4. Specific Surface Area

Specific surface area by the methylene blue method was determined according to the standard EN ISO 10545-4 [13]. Specific surface area is directly related to the rate of phyllosilicates [14]. The adsorption test is used to classify clays [15] [16].

2.5. Technological Tests

Drying curve (Bigot) was determined using a D124 barellatographe apparatus while dilatometer curve is carried out using a dilatometer Adamel Lhomargy type BI. The registration was completed when the drying recording of clay is not accompanied by shrinkage. Drying and dilatometric curves allow highlighting the variations in weight and volume as a function of temperature [17].

For the manufacture of bricks, different bricks underwent a drying operation performed in the open air and then in an oven at 100°C and firing was done by means of an electric furnace at various levels of temperature 800°C, 850°C, 900°C and 950°C. The rise of temperature increased from 30°C/h. For the manufacture of tiles, different tiles underwent a heating operation in an electric furnace at different temperatures 850°C, 900°C, 950°C and 1000°C with a gradient of 300°C/h. The determination of water absorption and flexural strength were carried out following the Standards [18] [19].

3. Experimental Results

3.1. Mineralogical Analysis

The results of mineralogical analysis (Figure 2) showed a clear change in the bottom to the top of the outcrops which distinguishes three mineralogical units (Table 1).

The unit A Mkt consisted mainly by illite and low smectite and Kaolonite. The H Mkt was marked by the

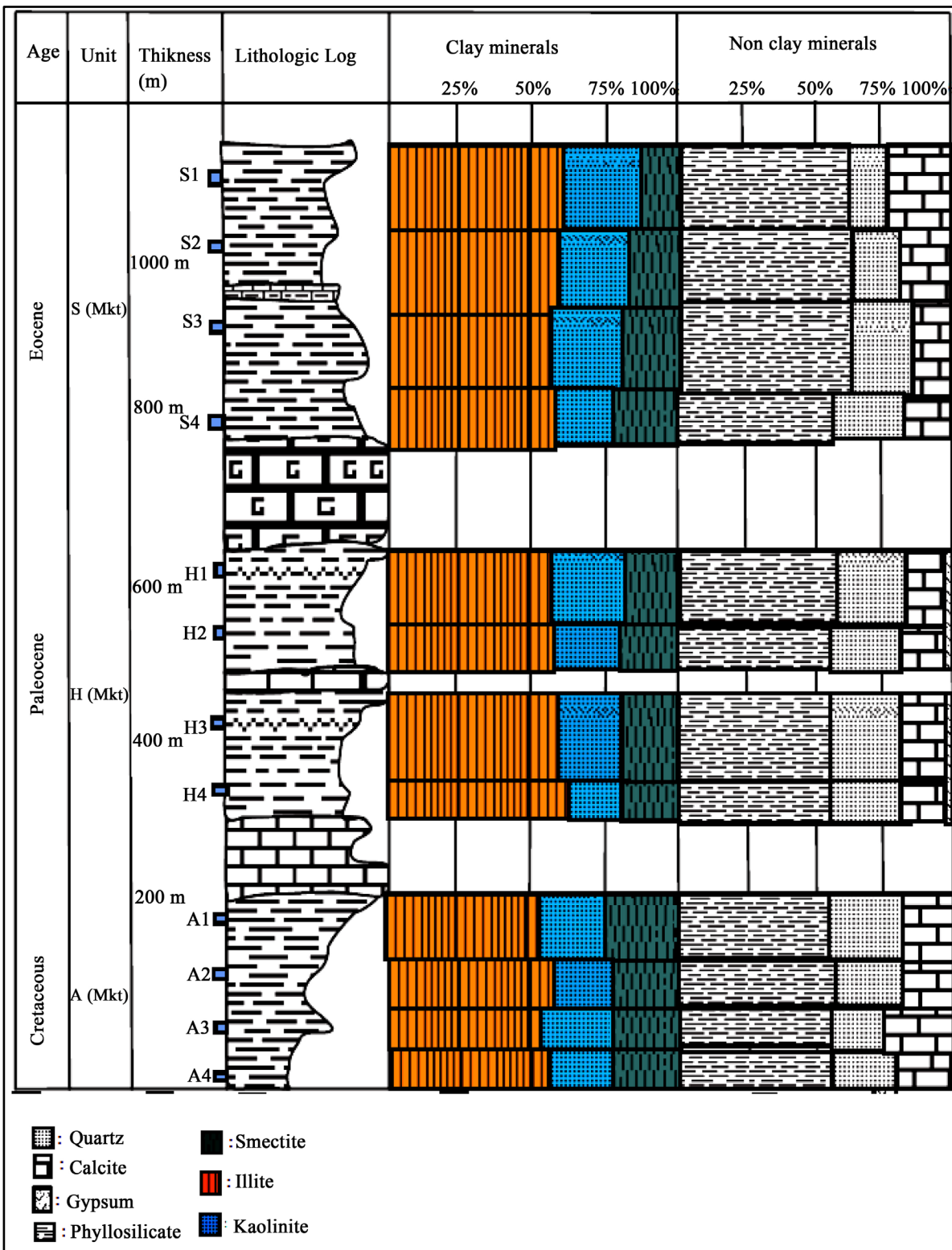


Figure 2. Mineralogical distribution of Makthar's clay.

increase in the content of illite and the percentage of smectite. The unit S Mkt was marked by the presence of illite and the kaolinite. Associated minerals were present at levels nearly homogeneous throughout the outcrops

Table 1. Mineralogical composition of total samples.

Unit	Samples	Total (bulk) sample				<2 μm Fraction		
		Phyllosilicate	Quartz	Calcite	Gypsum	Illite	Kaolinite	Smectite
Unit 3	S1 Mkt	62	15	23	-	62	25	13
	S2 Mkt	64	13	23	-	60	22	18
	S3 Mkt	64	17	19	-	58	25	17
	S4 Mkt	61	20	19	-	61	21	18
Unit 2	H1 Mkt	60	16	23	1	55	30	15
	H2 Mkt	61	15	22	2	52	32	16
	H3 Mkt	62	11	25	2	50	31	19
	H4 Mkt	62	11	25	2	54	30	16
Unit 1	A1 Mkt	55	25	20	-	65	20	15
	A2 Mkt	59	22	19	-	64	19	17
	A3 Mkt	58	17	25	-	62	19	19
	A4 Mkt	58	20	22	-	65	19	16

and were mainly represented by calcite and a percentage of quartz. Mineralogical results showed the dominance of illite presenting favorable properties for ceramic use. The content of quartz was very tolerable since it can be easily digested by vitreous flow during firing operation [20].

3.2. Chemical Analysis

Chemical analysis of the major elements was performed on a mixture of clays (Table 2). The results showed high content of CaO and Fe₂O₃. The percentage of SiO₂ indicated the importance of detrital contribution. Al₂O₃ had a relatively low percentage. Its origin cannot be the tetrahedral layer of clay minerals. The K₂O content was very high; it's probably related to the presence of micas. Levels of alkaline fluxes (Na₂O and K₂O) present high level for all clay mixture due to the relatively larger amount of illite and orthoclase [21]. By comparing this clay with a fireclay, whose alumina rate was higher than 45%, the alkaline fluxes lower than 4%, it can be remarked that the clay of Makthar area was very plastic and was cooked red since the percentage of Fe₂O₃ is higher than 1.5%. The problem of sulfur will be corrected by the addition of barium carbonate to the paste, which will form a more stable barium sulfate. The high loss on ignition (17%) associated with low SiO₂ and high Al₂O₃ contents were due to the significant content of clay minerals. Besides its fluxing role, Fe₂O₃ also provides the fired products the characteristic reddish colour. However, Fe₂O₃ is not the only factor responsible for the coloration of ceramic wares, as also other constituents such as CaO, MgO, MnO and TiO₂ can appreciably modify the colour of fired clays [22]. The temperature of firing, the amount of Al₂O₃ relative to a range of other constituents, and the furnace atmosphere all play an important role in the development of colour in the fired clay products [23].

3.3. Granulometric and Microgranulometric Analysis

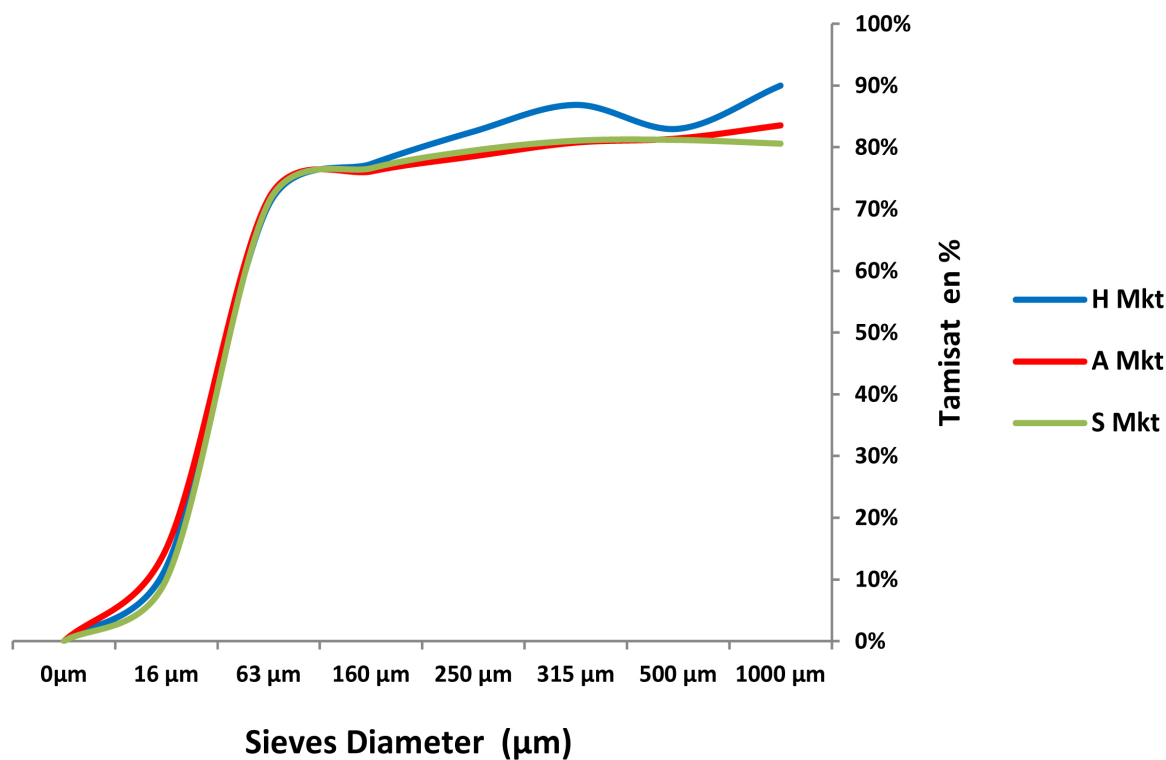
The particle size distribution of clay is a factor in determining its suitability for various applications, and particular attention should be given to the finer fraction (<2 μm) for ceramic products [9]. Granulometric analysis of clay indicated a homogeneous distribution. These results showed that the clay samples had sand fraction about 15% for unit A Mkt, 9% for the H Mkt and 5% for unit S Mkt. The percentage of elements whose diameter higher than 50 μm was negligible and approximately reached 5% for all units (Figure 3).

The microgranulometric analysis of clay mixtures showed that the elements whose diameter was lower than 2 μm was very high and reached 30%, for the unit H Mkt, 37% for the unit A Mkt and 35% for the unit S Mkt. The granulometry of all studied clays was excellent for use in ceramics. The problem arising by the presence of particles in the coarse sand fraction (200 - 2000 μm) can be solved simply by grinding.

The micro-size curves (Figure 4) for clay units H Mkt and A Mkt showed a parabolic facies indicating a

Table 2. Clay's chemical analysis.

Clay		L.O.I %	CaO %	Al ₂ O ₃ %	Fe ₂ O ₃ %	SiO ₂ %	MgO %	SO ₃ %	K ₂ O %
A Mkt	A1	17.64	7.49	17.48	7.88	36.47	3.63	0.08	1.11
	A2	13.95	8.54	8.61	7.52	37.94	2.76	1.8	0.88
	A3	23.48	2.73	12.25	9.22	43.58	2.89	0.02	1.88
	A4	14.36	8.76	8.64	7.47	37.6	2.70	1.83	0.87
H Mkt	H1	22.41	26.64	7.5	5.86	31.35	0.5	3	0.47
	H2	31.29	24.21	16.55	3.87	20.29	0.2	0.8	0.55
	H3	12.90	20.0	15.91	2.63	47.59	0.86	0.13	0.53
	H4	20.86	26.29	9.33	6.08	38.99	1.95	2.99	0.51
S Mkt	S1	23.48	26.0	14.79	2.52	23.42	1.46	0.09	0.93
	S2	22.54	25.17	14.85	2.54	22.89	1.35	0.09	0.92
	S3	24.84	28.36	18.82	3.64	37.3	1.52	1.72	0.58
	S4	21.34	27.11	18.69	3.71	32.01	1.62	1.88	0.54

**Figure 3.** Granulometric curves of different mixture clay of Makthar area.

transport operation either by turbidity currents at medium speed or by suspension graduated suspension [24].

3.4. Plasticity Tests

The values of the limits of plasticity and plasticity index values indicated that all mixture clay of Makthar area plastic-type (Table 3). These clay mixtures were located in the area of illitic minerals as shown on Holtz and Kovacs diagram (Figure 5). This is of importance for applications since it indicated the minimum moisture content necessary to reach a plastic condition. At a high plastic limit, the samples were more difficult to dry. On

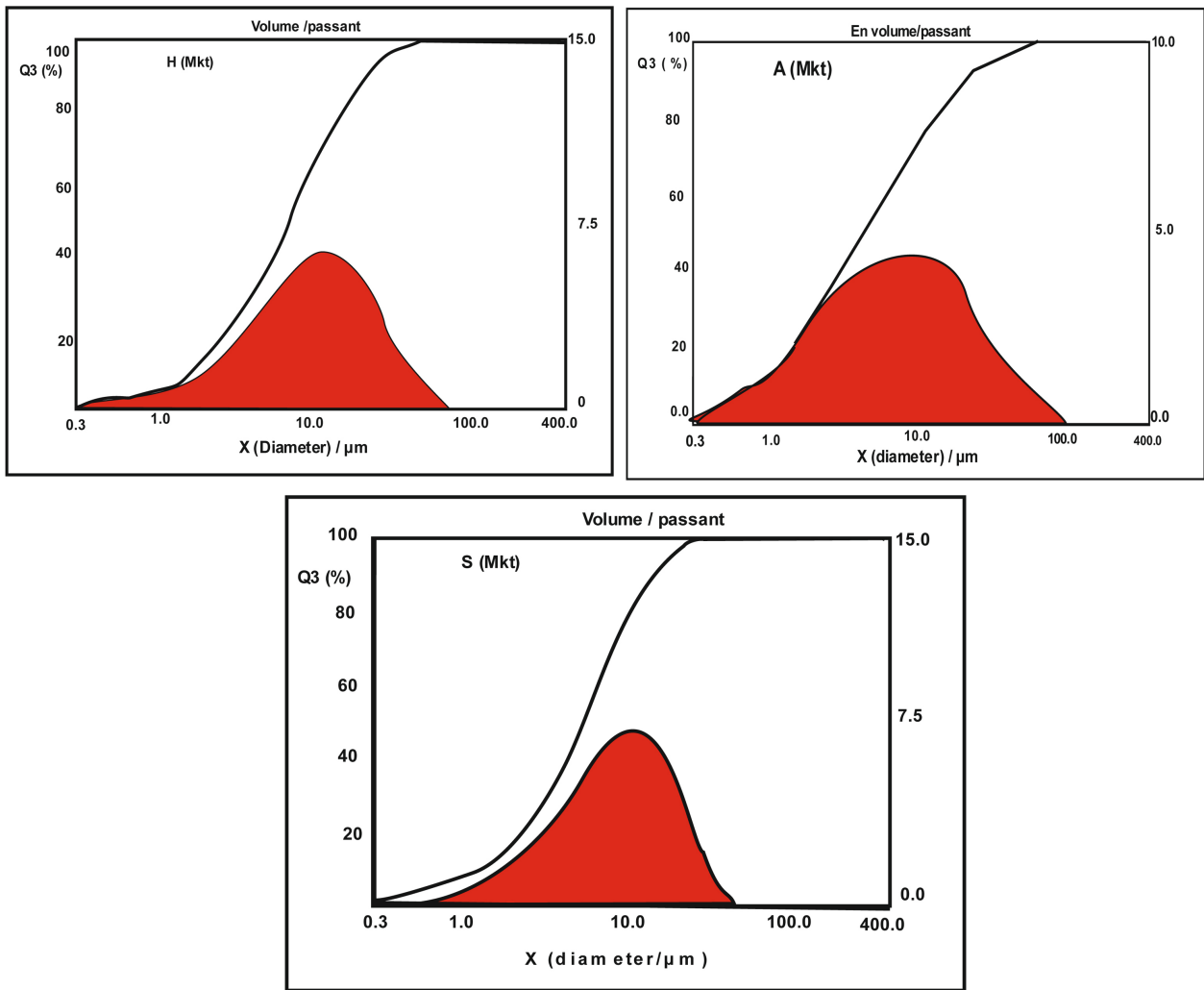


Figure 4. Micro-granulometric curves of different mixture clay of Makthar area.

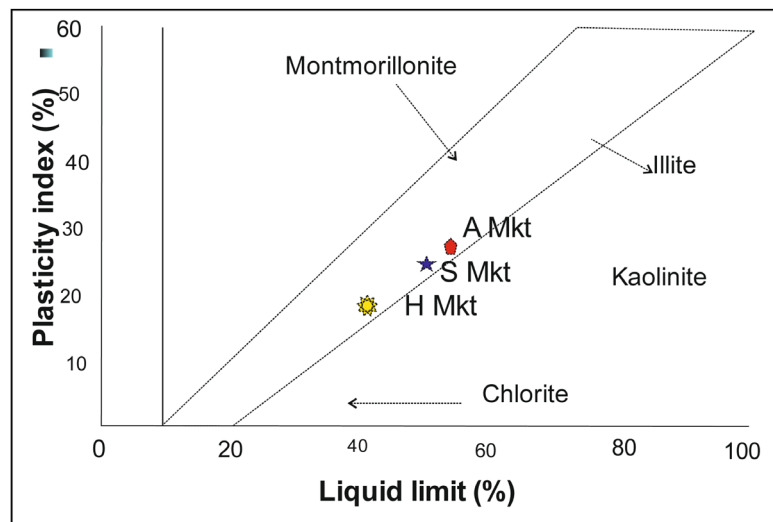


Figure 5. Position of the studied clays on the Holtz and Kovacs diagram.

Table 3. Plasticity of mixture clay of Makthar area.

Units	References	WL	Wp	Ip	Plasticity field
U1	A Mkt	54.34	36.05	26.28	Plastic clay
U2	H Mkt	42.75	26.35	18.39	
U3	S Mkt	57.83	32.77	25.05	

the other hand, the use of high plastic clays reduced the wearing down of the equipment for grinding and conformation (extruder). High plasticity was associated with bodies with greater mechanical strength [21]. **Figure 5** shows the position of these clays on the Holtz and Kovacs diagram [25]. The almost same PI value for all clays may be related to higher plastic limit of illite (35% - 60%) and montmorillonit (50% - 100%) than kaolinite (25% - 40%) [26].

3.5. Specific Surface Area

The mixture of clays of all clay units had specific surface which reflect illitic character (**Table 4**). We noted that the value of the specific surface was strongly influenced by the nature of the clay minerals and associated minerals. However, the presence of high levels of calcium carbonate can significantly diminish the value of the specific surface.

3.6. Drying and Cooking Behavior

3.6.1. Bigot Curve

The results of drying curves for the mixtures studied are shown in **Figure 6**. For each unit, the drying behavior is performed on mixtures formed by clay samples. The clay mixture A Mkt unit had a percentage of total water of 25.14%. The percentage of interposed water was 5.14%, while the percentage of colloidal water was 20%. The final drying shrinkage was 5.7%. The clay mixture of the H Mkt showed a percentage of total water of 28.44%. The percentage of interposed water was 8.44% and the percentage of colloidal water was 20%. The final drying shrinkage was 6.8%. The clay mixture of S Mkt unit had a percentage of total water of 31%. The percentage of interposed water was 10.4% while the percentage of colloidal water was 20.6%. The final drying shrinkage was 7.2%. The different results obtained indicated that different clays were preparing quick-drying.

3.6.2. Dilatometric Curves

The dimensional changes observed after firing of the raw clays are given in **Figure 7**. For the unit A Mkt showed that from ambient temperature to 110°C, developed a slight dilation which didn't not exceed 0.2%, this was due to desorption of adsorbed water. This expansion was followed by larger changes between 500 and 600°C due to the $\alpha \rightarrow \beta$ -quartz transformation. This dilation reached 2.2% at temperature 750°C (segment AB). Singer and Singer (1963) point out that α -quartz transformed into β -quartz at 573°C with a volume increase of 2% and on further slow heating β -quartz changed to $\beta 2$ -tridymite at 870°C with a volume increase of 12%. The maximum expansion rate between 500°C and 600°C was 583°C. After a slight shrinkage starting at around 850°C, a sharp shrinkage starting at 952°C was attributed to sintering and the formation of vitreous phases (segment BC). This mean interval of temperature gave the opportunity to the grains to react correctly between them and give materials that will resist to the deformation at high temperature, favorable asset for the ceramic production. This phenomenon deviated greater from 800°C to 1000°C indicating the end of fusible phase of the product (segment CD). The segment (DE) corresponded to the cooling. This curve was almost linear, indicating a cooking withdrawal of 1.6%. Dilatometric curve of the unit H Mkt showed that from ambient temperature to 120°C, developed a slight dilation of 0.2% followed by maximum dilation of 2.2% at 750°C (segment AB). From 750°C, there was the beginning of sintering phase (segment BC). This phenomenon deviated greater from 800°C to 900°C indicating the end of this phase (segment CD). The segment (DE) corresponded to the cooling phase indicating a final firing shrinkage of 2%. Dilatometric curve of the unit S Mkt showed that from ambient temperature to 120°C, developed a shrinkage of 0.5% followed by a maximum dilation of 2.3% at 800°C (segment AB). From 800°C, there was a gradual contraction and the beginning of the fusible phase (segment BC). This phenomenon deviated from 800°C to 870°C indicating the end of fusible phase (segment CD). The

Table 4. Specific surface area analysis.

Unit	Unit 1				Unit 2				Unit 3			
Samples (Mkt)	A1	A2	A3	A4	H1	H2	H3	H4	S1	S2	S3	S4
SSA (m ² /g)	112	178	176	180	210	220	235	255	250	265	270	230

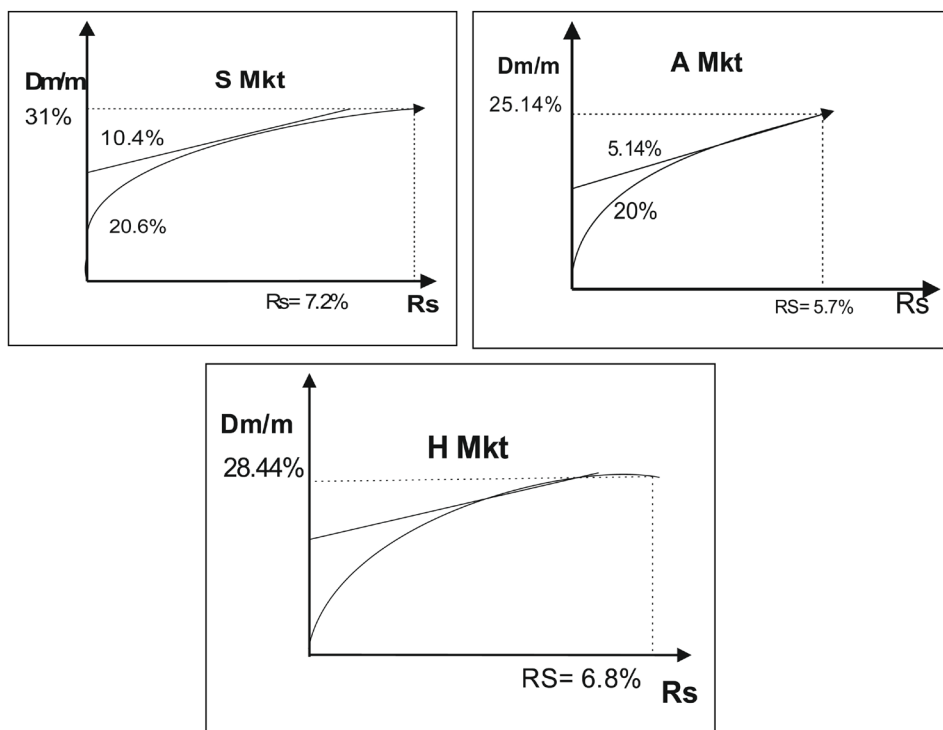


Figure 6. Drying curves of clay mixture of Makthar area: A Mkt, H Mkt and S Mkt.

segment (DE) corresponded to the cooling phase indicating a final firing shrinkage of 1.25%. The higher content of K₂O in all raw material, especially in <2 μm fraction, may contribute to the rapid vitrification.

3.6.3. Technological Tests for Bricks

Test results for manufacturing bricks are shown in Table 5. Drying shrinkage of the mixture clay of the unit A Mkt was almost of 5.7%, while for the two mixtures of H Mkt and S Mkt units, it was almost of 7%. Firing shrinkage of the product presented satisfactory values which depended on the temperature, and reached 2.27% for A Mkt, a value of 1.86% for the mixture H Mkt and a value of 1.37% for S Mkt at 950°C.

Loss of ignition increases slightly with the temperature and varies according to the presence of carbonates in the clays. It reached maximum values at 950°C. The percentage of loss on ignition was closely related to the molecular water, the oxidation of FeO, the decomposition of carbonates and the presence of organic matter. The water absorption varied inversely when the temperature increase, it decreased sharply to 10.11% for A Mkt, to 15.15% for H Mkt, and 12% for S Mkt to 950°C. All raw material mixture had almost color tending to red and yellow Figure 8. The increased redness and yellowness can be attributed to more amount of some oxide impurities. The different values and the red color appearance of the product were very tolerable which makes different material very profitable for industrial exploitation [27].

3.6.4. Technological Tests of Ceramic Tiles

For each temperature, we proceeded to heat five pieces of clay mixtures. The results are shown in Table 6. The flexural strength reaches 11 MPa to 12 MPa for all clay units at 1000°C. The mechanical resistance to the flexion increased with vitrification up to high level of resistance, then the material becomes breakable. For all clay

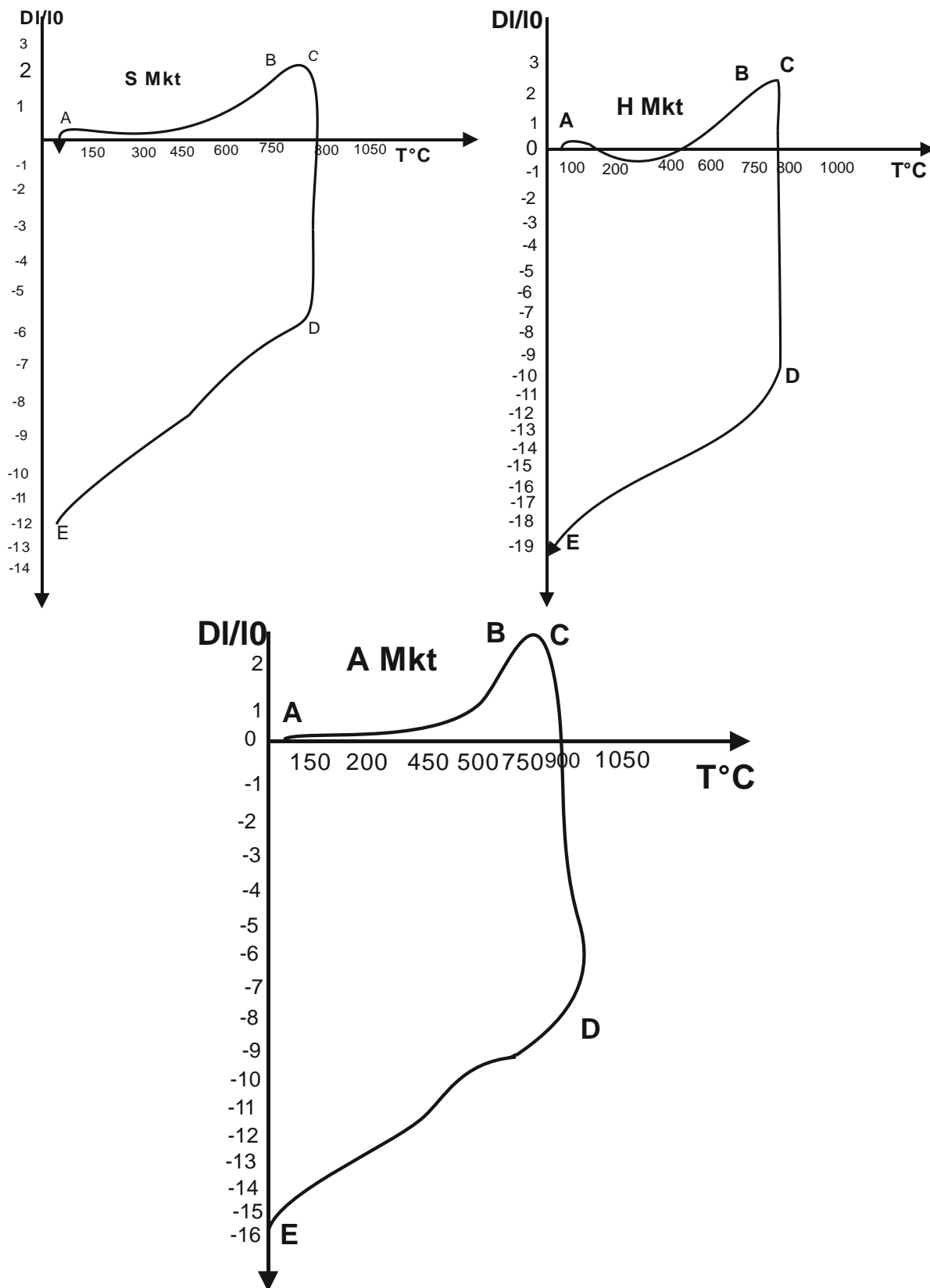


Figure 7. Dilatometric curves of clay mixture: A Mkt, H Mkt and S Mkt.

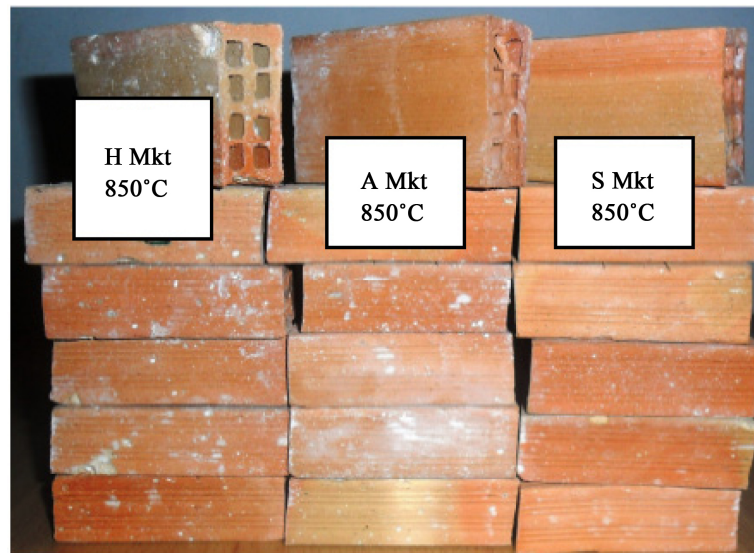


Figure 8. Different types of bricks from the clay of different section.

Table 5. Results of technological test of bricks.

Unit	Temperature °C	Drying Shrinkage (%)	Firing Shrinkage (%)	Loss of Ignition (%)	Water Absorption (%)
U1 (A Mkt)	800	5.7%	0.22	6.8	15
	850		0.40	6.9	13.9
	900		1.27	7	13.02
	950		2.27	7.53	10.11
U2 (H Mkt)	800	7%	0.03	17	15.9
	850		0.25	17.32	15.6
	900		1.43	18.12	15.5
	950		1.86	19.4	15.15
U3 (SMkt)	Lo	7.5%	0.06	17.4	16.17
	20.0		0.19	17.3	14.46
	20.0		1.13	17.8	12.12
	20.0		1.37	17.85	12.00

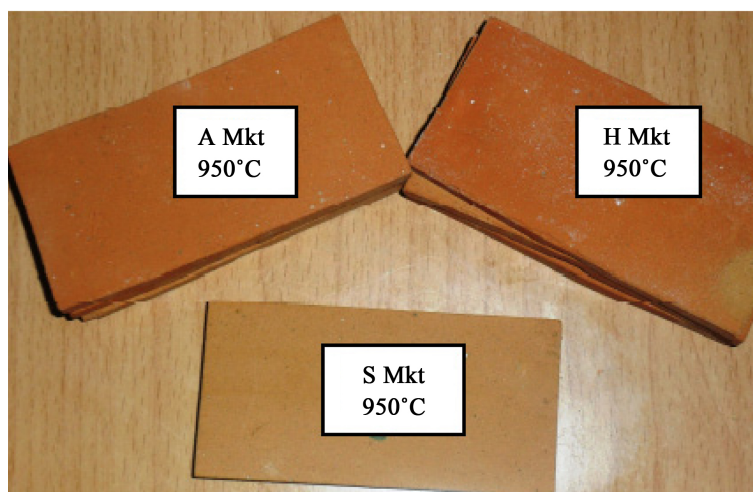
mixture, the temperature of 1000°C represented the limit of the mechanical resistance to the flexion. The firing temperature had an important effect on the mechanical strength of ceramic tile. The temperature increased the flexural strength due to densification. As the liquid phase reduced the porosity, which hinders crack formation and improved the mechanical strength. Higher proportions of orthoclase in the fraction $<2 \mu\text{m}$ of raw material favored vitrification and improved resistance of fired samples.

Above 900°C, the values of water absorption decreased and the amount of the liquid phase increased. This phase penetrated into the pores, closing them and isolating neighbouring pores. The liquid surface tension and capillarity helped to bring pores closer together and reduced porosity. This explains the intense decrease of the water absorption in this temperature range [28]. The firing shrinkage up to 1000°C was small around 1% for all raw materials.

Based on these results, these clays can be used in the field of manufacturing of bricks, without being broken or damaged by local constraints. However, technological tests of ceramic tiles showed that units A Mkt and S Mkt prepare well to get ceramic tile type B_{III} [29] (Figure 9). In contrast, the mixture of the H Mkt has some

Table 6. Results of technological test of tiles.

Unit	Temperature °C	Drying Shrinkage (%)	Firing Shrinkage (%)	Loss of Ignition (%)	Bending strength N/mm ²	Water Absorption %
U1 (A Mkt)	850	0.11%	0.3	7.2	2.3	10.73
	900		0.66	7.24	5.52	15.64
	950		0.90	7.13	10.21	16.98
	1000		0.90	7.6	10.52	18.73
U2 (H Mkt)	850	0.28%	0.5	17.2	3.3	26.18
	900		0.18	18.0	4.08	28.01
	950		0.08	19.8	4.8	30.4
	1000		0.02	20.0	5.25	31.7
U3 (SMkt)	850	0.25%	0.70	17.61	5.4	16.55
	900		0.85	17.99	9.42	18.88
	950		1.98	18.4	10.01	20.9
	1000		1.22	18.51	12.68	21.19

**Figure 9.** Different types of tiles from different clay sections.

defects which amount to a lifting surface (swelling). This defect may be remedied by increasing the rate of greaser remover [30].

4. Conclusions

Mineralogical analysis of clay mixture of Makthar area showed dominance of Illite with a small percentage of kaolinite and smectite. These clay minerals combined high content of calcite and quartz. This analysis showed relatively low values of the specific surface area and high values of plasticity index which confirmed the plastic character of clays according to the Casagrande diagram.

The geochemical analysis showed that the argillaceous series had a ratio of $\text{SiO}_2/\text{Al}_2\text{O}_3$ nearly 2. The K_2O content was almost 4% and the content of Fe_2O_3 was relatively large. The high percentage of CaO showed the enrichment of clay calcite and was confirmed by the high content of loss on ignition.

Technological Tests for bricks revealed a firing temperature of 900°C , a drying shrinkage of 7%, a weight loss of 20% and water absorption of 9%. However, technological tests for ceramic tiles, showed values of firing temperature of 1050°C , firing shrinkage of 0.25%, a flexural strength of 11 MPa and water absorption of 2%. The red color appearance obtained at the end of firing operation is favorable for use in ceramic industry despite

the presence of some defects which are easily remediable by chemical corrections.

Acknowledgements

Sincere thanks go to the staff of the Ceramic Laboratory of the technical center of construction materials, ceramic and glass (CTMCCV, Tunisia).

References

- [1] Ben Ayed, N. (1975) Etude géologique de cuvettes de Siliana et du Sers (Atlas Tunisien central). Thèse 3ème cycle, Université Pierre et Marie Curie, Paris, 82.
- [2] M'Rabet, A. (1987) Stratigraphie, Sédimentation et diagénèse carbonatée des séries Crétacé inférieur de la Tunisie Centrale. Thèse 3ème cycle, 412.
- [3] Burollet, P.F. (1973) Importance des facteurs salifères dans la tectonique tunisienne. *Annales de Minéralogie et de Géologie*, **26**, 110-120.
- [4] Castany, G. (1952) Paléogéographie, tectonique et orogénèse de la Tunisie. *XIXème Congrès géologique international*, Alger.
- [5] Turki, M.M. (1988) Polycinématique et contrôle sédimentaire associé sur la cicatrice Zaghouane-Nebhana. *Mémoire*, **7**, 252.
- [6] Srasra, E. (1987) Caractérisation minéralogique, propriétés physico-chimiques et application de l'argile de Haidoudi. Thèse de doctorat 3ème cycle, Faculté des Sciences de Tunis.
- [7] Amri, M. (1988) Inventaire des argiles smectitiques et leurs éventuelles utilisations dans l'industrie: Les smectites du Paléocène-Eocène inférieur dans les bassins du Centre-Ouest et du Sud-Ouest de la Tunisie. Thèse 3ème cycle, Faculté des Sciences, Tunis, 148.
- [8] Norme XP P 94-041 (1995) Identification granulométrique. Méthode de tamisage par voie humide.
- [9] Mahmoudi, S., Srasra, E. and Zargouni, F. (2008) The Use of Tunisian Barremian Clay in the Traditional Ceramic Industry: Optimization of Ceramic Properties. *Applied Clay Science*, **42**, 125-129. <http://dx.doi.org/10.1016/j.clay.2007.12.008>
- [10] Nahdi, K. (1997) Identification physico-chimique de l'argile de jebel Ressay. Application aux céramiques. Mémoire de D.E.A., Tunis, 86.
- [11] Norme NFP 94-051 (1993) Reconnaissance et essais. Détermination des limites d'Atterberg. Limite de liquidité à la coupelle. Limite de plasticité au rouleau.
- [12] GTR-LCPC (1987) Limites d'Atterberg, limite de liquidité, limite de plasticité, Méthodes d'essai. LCPC, 26.
- [13] Norme EN ISO 10545-4 (2012) Mesure de la quantité d'adsorption de bleu de Méthylène d'un sol ou d'un matériau rocheux par l'essai de tâche.
- [14] Jamoussi, F. (2001) Les argiles de la Tunisie: Etude minéralogique, géochimique, géotechnique et utilisations industrielles. Thèse d'État, université El Manar, Tunis.
- [15] GTR-LCPC (1992) Guide Technique pour la réalisation des remblais et des couches de forme.
- [16] GTR-LCPC (2000) Guide Technique pour le traitement du sol à la chaux et/ou aux liants hydrauliques.
- [17] Hachani, M. (2004) Caractérisation et valorisation des argiles du Crétacé inférieur du Jebel Zitoun (région de Krib) Tunisie Nord orientale. Mémoire Mastère en géologie appliquée, Université de Carthage, Tunis.
- [18] Norme ISO 10545-4 (2004) Carreaux et dalles céramiques—Partie 4: Détermination de la résistance à la flexion et de la force de rupture.
- [19] Norme ISO 10545-3 (2004) Carreaux et dalles céramiques—Partie 3: Carreaux et dalles céramiques—Détermination de l'absorption d'eau.
- [20] Ben Salah, I. (2003) Etude des matériaux utiles du Crétacé supérieur et du Paléogène de la Tunisie centrale (région de Makthar). Mémoire de Mastère, Faculté des Sciences de Tunis, 85, Tunis.
- [21] Monterio, S.N. and Vieira, C.M.F. (2004) Influence of Firing Temperature on the Ceramic Properties of Clays from Campos dos Goytacazes, Brazil. *Applied Clay Science*, **27**, 229-234. <http://dx.doi.org/10.1016/j.clay.2004.03.002>
- [22] Kreimeyer, R. (1987) Some Notes on the Firing Color of Clay Bricks. *Applied Clay Science*, **2**, 175-183. [http://dx.doi.org/10.1016/0169-1317\(87\)90007-X](http://dx.doi.org/10.1016/0169-1317(87)90007-X)
- [23] Fisher, P. (1984) Some Comments on the Color of Fired Clays. *Ziegel Industrie International*, **37**, 475-483.
- [24] Ben M'Barek, M. (1996) Identification et valorisation des argiles du Paléogène du Nord de la Tunisie et leurs

- applications industrielles. DEA, Faculté des Science de Tunis, 91.
- [25] Holtz, R.D. and Kovacs, W.D. (1981) Part 3: The Relationship between Geology and Landslide Hazards of Atchison, Kansas and Vicinity. Kansas Geotechnical Survey, *Current Research in Earth Science*, **244**, 733-808.
- [26] Mitchell, J.K. (1993) *Fundamentals of Soil Behavior*. 2nd Edition, John Wiley & Sons, Hoboken.
- [27] Cherni, R. (2008) Les argiles du Crétacé supérieur—Paléocène de la région Bir M'Chergua et de Jebel Kharouba. Bi-ostratigraphie et apports industriels. Diplôme Etudes Approfondies, Faculté Des Sciences de Bizerte, 98.
- [28] Baccour, H., Medhioub, M., Jamoussi, F. and Mhiri, T. (2009) Influence of Firing Temperature on the Ceramic Properties of Triassic Clays from Tunisia. *Journal of Materials Processing Technology*, **209**, 2812-2817.
<http://dx.doi.org/10.1016/j.jmatprotec.2008.06.055>
- [29] Ben M'Barek, M. (2001) Les argiles du Crétacé et du Paléogène du Nord Est de la Tunisie: Caractérisation et essais d'applications industrielles.
- [30] Handous, M.F. (1990) Etude céramique et essai industriel des argiles du Nord-Est de la Tunisie pour la fabrication de terre cuite. DEA, Faculté des Sciences de Tunis, 122.



Scientific Research Publishing

Submit or recommend next manuscript to SCIRP and we will provide best service for you:

Accepting pre-submission inquiries through Email, Facebook, LinkedIn, Twitter, etc.

A wide selection of journals (inclusive of 9 subjects, more than 200 journals)

Providing 24-hour high-quality service

User-friendly online submission system

Fair and swift peer-review system

Efficient typesetting and proofreading procedure

Display of the result of downloads and visits, as well as the number of cited articles

Maximum dissemination of your research work

Submit your manuscript at: <http://papersubmission.scirp.org/>